U.S. Department of the Interior
U.S. Geological Survey

USW H-5

Original Logs

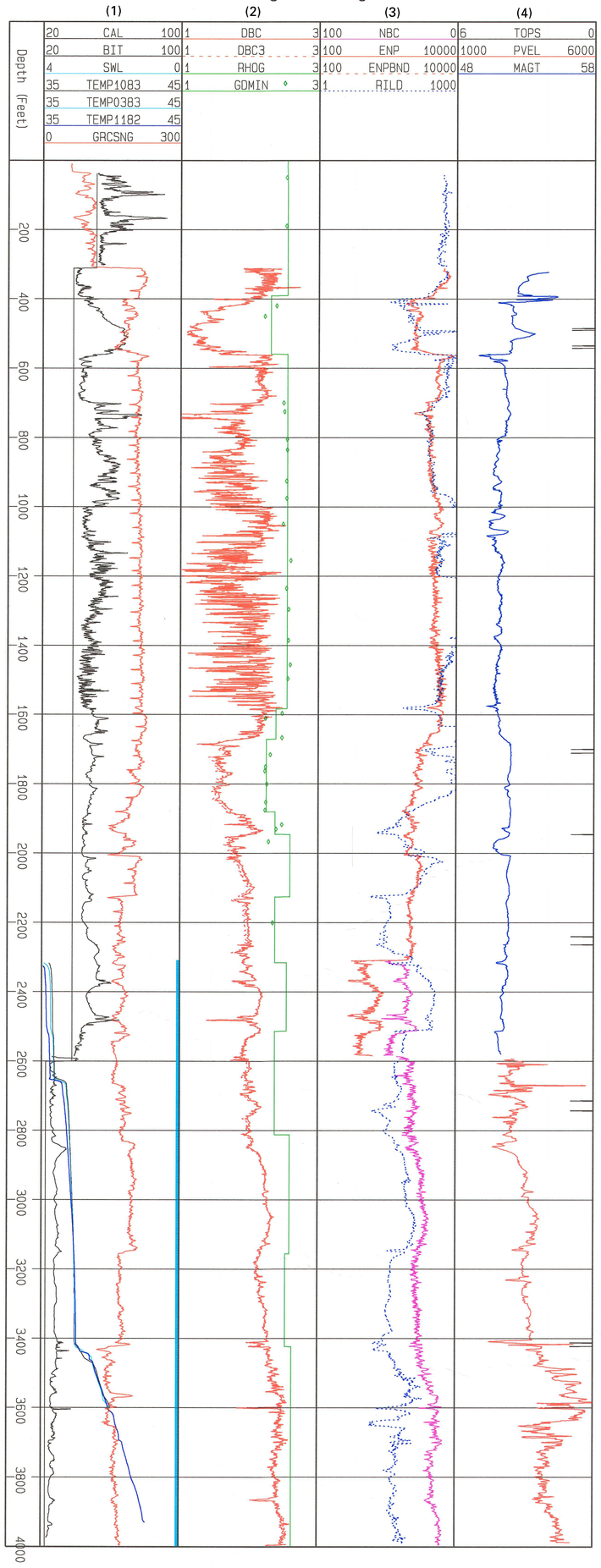

Porosity and Water Content

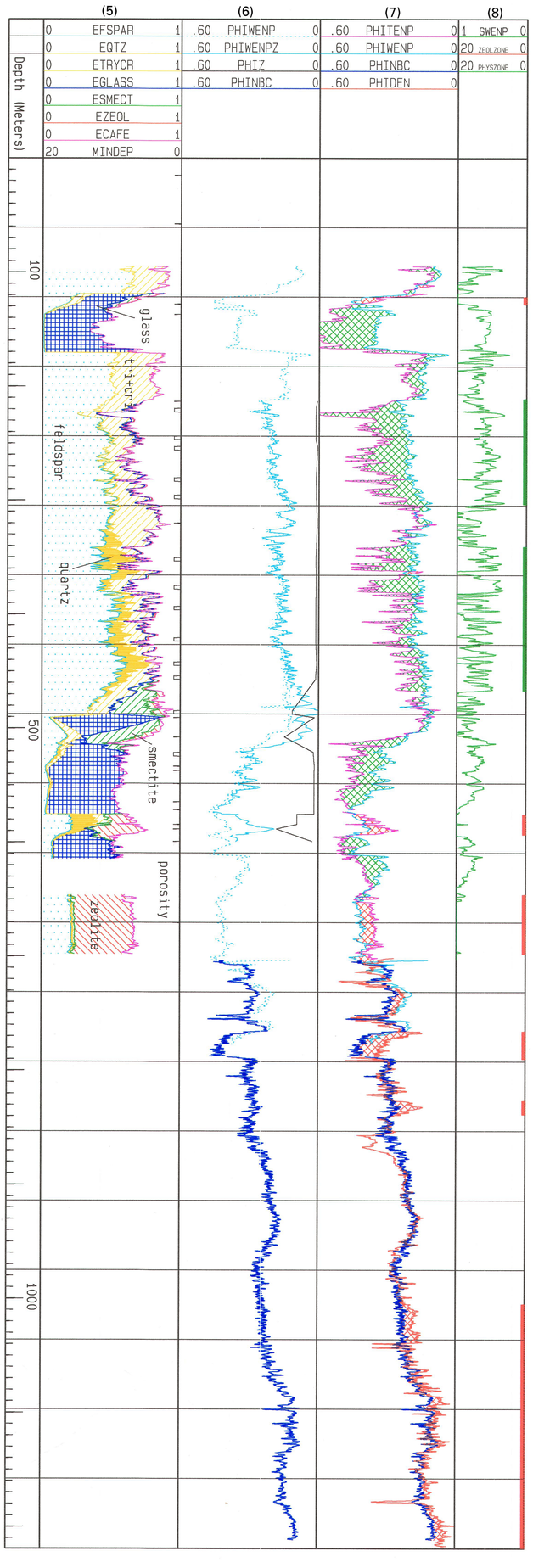

Stratigraphy, Fractures, and Flow

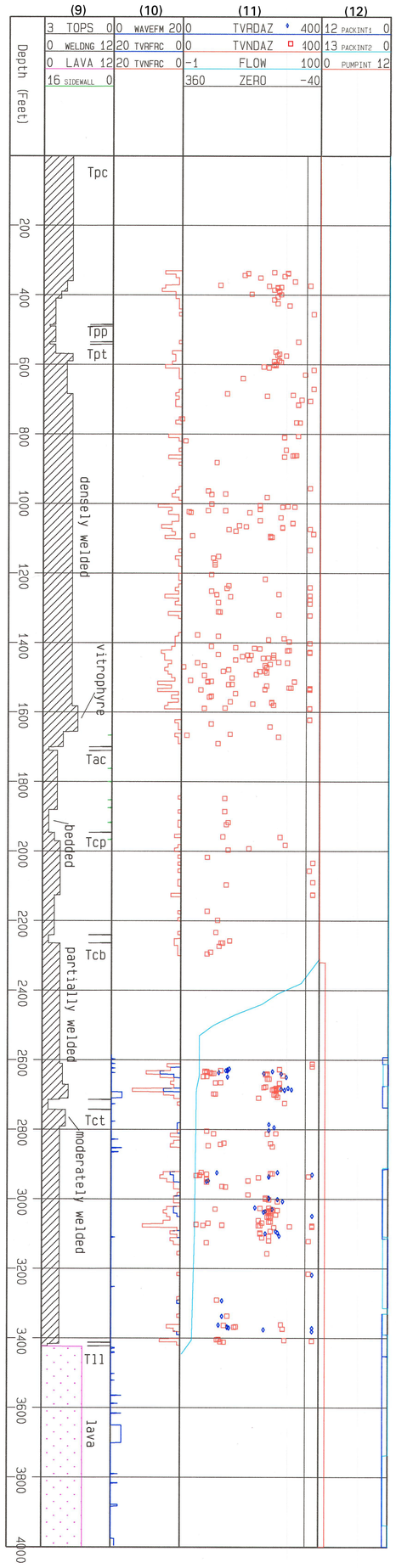

BOREHOLE USW H-5, YUCCA MOUNTAIN, NEVADA

Compiled by Philip H. Nelson and Joyce E. Kibler
U.S. Geological Survey, Denver, Colorado

Borehole H-5 was completed in June, 1982 to a total depth of 4000 feet. The hole was rotary drilled using air foam consisting of air, detergent, and water (Bentley et al., 1983). A few sidewall cores were obtained as indicated by ticks labelled sidewall in column 9. Depth on the plot is measured along hole, and has not been corrected for deviation. Hole deviation is slight, (Plate 12 in Nelson and others, 1991): at a true vertical depth of 3979.5 feet, the measured depth is 3980 feet and the horizontal offset is 42 feet.

Original logs in columns 1-4, acquired between May 25, 1982 and July 23, 1982, were described and presented by Nelson and others, 1991. Three temperature logs (Sass and others, 1988) obtained in November 1982, March 1983, and October 1983 also appear in column 1.

Mineralogy in column 5 is derived from X-ray diffraction data by Bish and Chipera (1989). Their data have been converted to volume percent, combined with porosity, and in several places extrapolated to boundaries inserted where marked changes in log response occur.

Estimates of total water content in column 6 are derived from the epithermal neutron log (phiwenp) and thermal neutron log (phinbc). Between 2310 and 2550 feet phinbc can be compared with phiwenp. Structural water phiz is estimated from mineralogy and subtracted from phiwenp to form an estimate of water in pore space, phiwenpz.

Porosity (phitenp, phiden) and water content (phiwenp, phinbc) are given in column 7. Phitenp and phiwenp were computed from epithermal neutron and density logs (Nelson, 1994). Green hatching between the porosity and water content curves denotes air-filled porosity. Red hatching appears where water content exceeds porosity, often indicating the presence of zeolitic minerals.

Saturation (column 8) is computed as the ratio of phiwenp to phitenp. The flags lithzone and physzone (green and red bars in column 8) denote the presence of abundant lithophysae and extensive alteration, respectively. Their depth extent is taken from inspection of the green and red hatch areas in column 7 and from other considerations.

Stratigraphic tops and degree of welding, given in column 9, are taken from Bentley and others, 1983.

Disruptions in the sonic waveform log (wavefm, column 10) are often due to fractures or faults. Temperature gradient logs, dtmp, were not computed due to the pronounced isothermal zones separated by discrete temperature increases, as exhibited in column 1. Plots of individual fractures, column 11, observed on televiewer (tvrdaz) and television (tvndaz) logs are plotted to show the azimuth of the dip of each fracture. The same data are plotted as fracture density (tvrfrc, tvnfrc) in column 10. The televiewer log was limited to the interval 2582 to 3449 feet.

A flow log (Bentley and others, 1983) shown in column 11 was derived from tracer tests carried out during a pump test. The flow log shows that 90 percent of total yield during the pump test came from the Bullfrog Tuff. The pumped interval is shown in column 12 as pumpint. A model used by Robison and Craig (1988) for the pump tests indicated a transmissivity of about 35 meters squared per day. Results of the packer injection tests were inconclusive, but the packer-test intervals are shown nevertheless (packint).

EXPLANATION OF CURVES AND SYMBOLS

Column 1
CAL Caliper in cm, black curve.
BIT Bit size in cm, black line.
SWL Static water level, vertical cyan bar.
TEMP Temperature in degrees C, three colors dated by month, year.
GRCSNG Gamma ray in API units, casing effect removed, red curve.

Column 2
DBC Density in g/cm3, red curve.
DBC3 Density bound in g/cm3, red dash curve.
RHOG Grain density in g/cm3, green curve.
GDMIN Grain density from mineralogy, green diamonds.

Column 3
ENP Epithermal neutron in counts/sec, red curve.
ENPBND Epithermal bound, red dash curve.
NBC Thermal neutron log in porosity, magenta curve.
RILD Induction resistivity in ohm-m, blue dot.

Column 4
PVEL Compressional-wave velocity in m/s, red curve.
MAGT Total magnetic field in microTesla, blue curve.
TOPS Stratigraphic boundaries, black ticks.

Column 5 [shaded areas represent volume fractions]
EFSPAR Feldspar, blue dotted area to left-hand edge.
EQTZ Quartz, dark yellow area.
ETRYCR Tridymite + cristobalite + opal, light yellow.
EGLASS Glass, blue gridded area.
ESMECT Smectite + kaolinite, green slanted area.
EZEOL Clinoptilolite + mordenite + analcime, red slant.
ECAFE Calcite + hornblende + hematite + chlorite, magenta hatch.
Porosity Unshaded area to the right-hand edge.
MINDEP Depth of x-ray diffraction samples, ticks.

Column 6 [fractional volume of whole rock, increasing to left]
PHIWENP Water-filled porosity, from ENPBND and DBC3 logs, cyan curve.
PHIWENPZ Water-filled porosity, structural water removed.
PHIZ Structural water, black curve.
PHINBC Water content from corrected NBC, blue curve.

Column 7 [fractional volume of whole rock, increasing to left]
PHIWENP Water-filled porosity, from ENPBND and DBC3 logs, cyan dot curve.
PHITENP Porosity, from ENPBND and DBC3 logs, magenta curve.
(green hatch where PHITENP > PHIWENP, red where PHITENP < PHIWENP).
PHIDEN Porosity, computed from DBC3 log, red curve.
(red hatch where PHIDEN < PHINBC).
PHINBC Water content from NBC, blue curve.

Column 8
SWENP Water saturation, ratio of PHIWENP to PHITENP, green curve.
PHYSZONE Lithophysal zone, picked from logs, green bar.
ZEOLZONE Zeolitic zone, picked from logs, red bar.

Column 9
TOPS Stratigraphic boundaries, black ticks.
WELDNG Degree of welding from core inspection, black slant.
LAVA Lava, magenta fill with dotted symbol.
SIDEWALL Location of sidewall samples, green ticks.

Column 10
WAVEFM Disruptions in sonic waveform log, blue ticks and bars.
TVRFRC Number of fractures per 10 feet, from televiewer, blue.
TVNFRC Number of fractures per 10 feet, from television, red.

Column 11
FLOW Flow log from tracer tests while pumping, cyan curve.
TVRDAZ Dip azimuth of fractures, from televiewer, blue diamonds.
TVNDAZ Dip azimuth of fractures, from television, red squares.
Undetermined azimuth is coded as 380 or 390 degrees.

Column 12
PACKINT1, 2 Intervals of packer injection tests, blue, cyan lines.
PUMPINT Intervals of pump tests, red lines.

Stratigraphic Names
[Unmarked ticks are bedded units]

-Paintbrush Group-
Tpc Tiva Canyon Tuff
Tpp Pah Canyon Tuff
Tpt Topopah Spring Tuff

Tac Calico Hills Formation

-Crater Flat Group-
Tcp Prow Pass Tuff
Tcb Bullfrog Tuff
Tct Tram Tuff

Tll Flow breccia and lava

NOTES

Date of last computation: October 1995
Plot Date: November 1995
Scientific Notebook: SN-0092

REFERENCES

Bentley, C. B., Robison, J. H., and Spengler, R. W., 1983, Geohydrologic data for well USW H-5, Yucca Mountain area, Nye County, Nevada: U.S. Geological Survey Open-File Report 83-853.

Nelson, P.H., Muller, D.C., Schimschal, U., Kibler, J.E., 1991, Geophysical logs and core measurements from forty boreholes at Yucca Mountain, Nevada: Geophysical Investigations Map GP-1001, 64 p., 40 plates.

Nelson, P.H., 1994, Saturation levels and trends in the unsaturated zone, Yucca Mountain, Nevada, Proceedings of the Fifth Annual International Conf. on High Level Radioactive Waste Management, Las Vegas, v. 4, p. 2774-2781.

Robison, J.H., and Craig, R.W., 1988, Geohydrology of rocks penetrated by test well USW H-5, Yucca Mountain area, Nevada: U.S. Geological Survey Water-Resources Investigations Report 88-4168, 44 p.

Sass, J. H., Lachenbruch, A. H., Dudley, W.W., Jr., Priest, S.S., and Munroe, R.J., 1988, Temperature, thermal conductivity, and heat flow near Yucca Mountain, Nevada: Some tectonic and hydrologic implications: U.S. Geological Survey Open-file Report 87-649, 118 p.

Petrophysical Properties, Mineralogy, Fractures, and Flow Tests in 25 Deep Boreholes at Yucca Mountain, Nevada

By Philip H. Nelson and Joyce E. Kibler

ISSN 2331-1258 (online)
http://dx.doi.org/10.3133/ofr20141023